

## Synthesis and Characterization of SnO<sub>2</sub> Nanoparticle by Microwave Assisted Hydrothermal Method

E. Brightlin Felcia<sup>1</sup>, K. Dhinakar Gnanam<sup>2</sup>

<sup>1</sup>(physics, St. John's College/MS University, India)

<sup>2</sup>(St. John's College/MS University, India)

---

**Abstract:** The proposed project work is to synthesis SnO<sub>2</sub> nanoparticles by microwave assisted hydrothermal method. We have used two solvents to synthesis SnO<sub>2</sub> nanoparticles and comparing the structural and optical characteristics. The prepared samples are annealed with 250, 500 and 750 for one hour. The structural parameters are studied using XRD spectrum. The optical characterizations are performed using FTIR spectroscopy and UV-Vis spectroscopy. The band gap values of the samples are calculated using tauc plot.

**Keywords:** Tin oxide, XRD, UV-VIS, FTIR

---

### I. Introduction

Metal oxides play a very important role in many areas of chemistry and materials science due to its ability to adopt vast number of structural geometries with an electronic structure that can display metallic, semiconductor or insulator properties [1]. Semiconductor nanoparticles have been a topic of great interest because of their excellent electrical, optical and magnetic properties. Due to cluster size reduction, the quantum confinement of charge carriers inside nanoparticles results in a blue shift of the band gap [2]. SnO<sub>2</sub> is one of the n-type semiconductor oxide with wide band gap of 3.6 eV [3]. The simultaneous occurrence of transparency and conductivity of SnO<sub>2</sub> is a unique feature among the group-IV elements of the periodic table [4]. SnO<sub>2</sub> has high electron mobility as well as large third-order nonlinear optical susceptibilities in the form of thin film [5]. Due to wide band gap, SnO<sub>2</sub> possesses high carrier density, oxygen vacancy and excellent optical and electrical properties [6]. SnO<sub>2</sub> is widely used in extensive range of applications like gas sensors, heat reflecting mirrors, varistors, transparent electrodes for solar cells, glass melting electrodes, optoelectronic devices, and photo electrode materials in high performance dye-sensitized solar cells (DSSC) [7–9], lithium rechargeable batteries, electrochromic windows [10], and catalysis [11, 12]. Therefore, the synthesis of fine SnO<sub>2</sub> nanoparticles is very important for their basic research and applications. In this work, microwave-assisted chemical route method is utilized for the synthesis of SnO<sub>2</sub> [13–17]. Due to uniform heating of the solutions, this method has significant advantages for its very short processing time, good control over particle size [18] and uniform nucleation of nanocrystals to achieve a narrow size distribution of SnO<sub>2</sub>.

### II. Experimental

#### 2.1 synthesis of tin oxide:

The SnO<sub>2</sub> nanoparticles are synthesized using microwave assisted hydrothermal method. This method have many advantages. With microwave heating, the energy can be applied directly to the sample rather than conductively, via the vessel. Heating can be started or stopped instantly, or the power level can be adjusted to match the required. Microwave dielectric heating is a non-quantum mechanical effect and its leads to volumetric heating of the samples. The SnO<sub>2</sub> nanoparticles are synthesized using microwave assisted hydrothermal method. [19] The precursors used for the synthesis of SnO<sub>2</sub> were analytical grade Tin (II) chloride, urea as a catalyst and water as solvent. Initially at room temperature, Tin (II) chloride and urea were dissolved in ethylene glycol by constant stirring for 90 min in a magnetic stirrer. The microwave power was set of 650 watt and operated at the rate of 2 minutes per cycle and cooled between the intervals until the precipitate was formed. The resulting precipitate was washed with double distilled water and dried. Again, the dried powders were washed with acetone and annealed at 250 °C, 500 °C and 750 °C for 1 hr in air atmosphere to remove unwanted organic substances present if any. The SnO<sub>2</sub> nanoparticles are synthesized using microwave assisted hydrothermal method. The precursors used for the synthesis of SnO<sub>2</sub> were analytical grade Tin (II) chloride, urea as a catalyst and ethylene glycol as solvent. Initially at room temperature, Tin (II) chloride and urea were dissolved in ethylene glycol by constant stirring for 90 min in a magnetic stirrer. The microwave power was set of 650 watt and operated at the rate of 2 minutes per cycle and cooled between the intervals until the precipitate was formed. The resulting precipitate was washed with double distilled water and dried. Again, the dried powders were washed with acetone and annealed at 250 °C, 500 °C and 750 °C for 1 hr in air atmosphere to remove unwanted organic substances present if any.

### III. Characterization Techniques

#### 3.1 Powder X-ray diffraction Pattern

##### 3.1.1 XRD Spectrum Analysis of SnO<sub>2</sub> Nanoparticles Synthesized Using water as Solvent

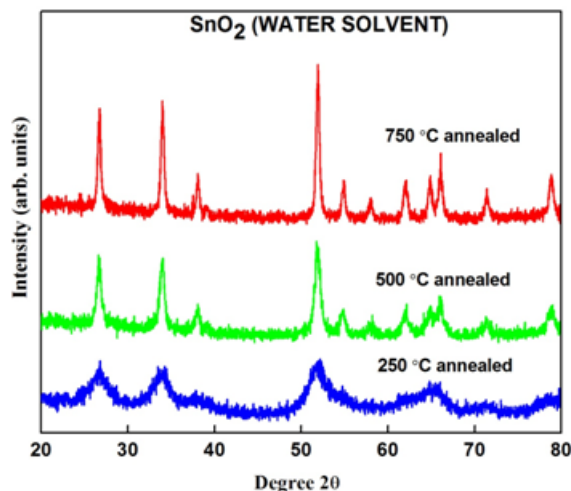


**Fig. 3.1** XRD patterns of 250 °C, 500 °C and 750 °C annealed SnO<sub>2</sub> samples synthesized using water as solvent.

Fig. 3.1 shows the XRD patterns of 250 °C, 500 °C and 750 °C annealed SnO<sub>2</sub> samples synthesized using water solvent. The average crystallite size (*D*) is calculated using Scherrer's formula presented in equation (1)

$$D = \frac{0.9\lambda}{\beta \cos \theta} \tag{1}$$

Where  $\lambda$ ,  $\beta$  and  $\theta$  are the wavelength of X-ray used, full width at half maximum and Bragg's angle respectively.

The XRD patterns of 250 °C annealed sample have four peaks and the peaks are also not clear. The intensities of the peaks are very small but the peaks are broad. The particle size and the FWHM values and the corresponding hkl values are tabulated in the Table 1. The peaks are matched with the JCPDS card number 72 – 1147. The major peaks are in the position of 26.91°, 33.91°, 52.29°, 65.04°. All the peaks have been indexed to tetragonal crystal structure of SnO<sub>2</sub>. It belongs to P<sub>4</sub>/mnm space group. The increase in full width half maximum and decrease in intensity of the peak denote the not as much of crystallinity of SnO<sub>2</sub> nanoparticles. [20-26] The average particle size of the samples are found as 4.566nm.

The XRD patterns of 500 °C annealed sample have seven peaks and the peaks are clear. The intensities of the peaks are increased while compared with the 250 °C annealed sample this indicates that the crystallinity of the sample gets increased. The particle size and the FWHM values and the corresponding hkl values are tabulated in the Table 2. The peaks are matched with the JCPDS card number 72 – 1147. The major peaks are in the position of 26.60°, 34.10°, 38.11°, 51.70°, 54.87°, 62.05°, 78.72°. All the peaks have been indexed to tetragonal crystal structure of SnO<sub>2</sub>. It belongs to P<sub>4</sub>/mnm space group. The decrease in full width half maximum and increase in intensity of the peak denote the good crystallinity of SnO<sub>2</sub> nanoparticles. The average particle size of the samples are found as 12.181nm. The value of the average particle size increased due to the increase in annealing temperature.

The XRD patterns of 750 °C annealed sample have eleven peaks and the peaks are clear. The intensities of the peaks are increased while compared with the 250 °C and 500 °C annealed samples and this indicates that the crystallinity of the sample gets increased. The particle size and the FWHM values and the corresponding hkl values are tabulated in the Table 3. The peaks are matched with the JCPDS card number 72 – 1147. The major peaks are in the position of 26.76°, 33.97°, 38.14°, 51.82°, 54.81°, 57.98°, 61.99°, 64.76°, 66.16°, 71.38°, 78.88°. All the peaks have been indexed to tetragonal crystal structure of SnO<sub>2</sub>. It belongs to P<sub>4</sub>/mnm space group. The decrease in full width half maximum and increase in intensity of the peak denote the good crystallinity of SnO<sub>2</sub> nanoparticles. The average particle size of the samples are found as 19.497nm. The value of the average particle size increased due to the increase in annealing temperature.

**Table 1.** Structural Parameters Of SnO<sub>2</sub> Nanoparticles Annealed With 250 °C Using Water Solvent.

S.No	Peak Position	hkl value	D spacing	FWHM	Particle Size(nm)
1	26.9169	110	3.34967	2.0188	4.02905
2	33.9169	101	2.63648	1.8303	4.51834
3	52.2923	211	1.76471	1.7634	4.99689
4	65.0422	112	1.43417	1.9864	4.72219

**Table 2.** Structural parameters of SnO<sub>2</sub> nanoparticles annealed with 500 °C using water solvent

S.No	Peak Position	hkl value	D spacing	FWHM	Particle Size(nm)
1	26.6059	110	3.34022	0.6468	12.5675
2	34.1003	101	2.63382	0.6199	13.3475
3	38.1119	200	2.36183	0.7469	11.2049
4	51.7014	211	1.76464	0.6022	11.663

5	54.8733	220	1.67549	0.6433	13.8538
6	62.0568	310	1.49682	0.7991	11.5504
7	78.7250	321	1.41340	0.9231	11.0808

**Table 3.** Structural parameters of SnO<sub>2</sub>nanoparticles annealed with 750 °C using water solvent

S.No	Peak Position	hkl value	D spacing	FWHM	Particle Size(nm)
1	26.7614	110	3.33557	0.4354	18.6626
2	33.9760	101	2.63634	0.3963	20.8712
3	38.1430	111	2.36242	0.3945	21.216
4	51.8258	211	1.75875	0.4650	18.9116
5	54.8111	220	1.67086	0.4606	19.3437
6	57.9831	002	1.58985	0.5495	16.4563
7	61.9946	310	1.49717	0.5587	16.5152
8	64.7623	112	1.43785	0.4320	21.6796
9	66.1617	301	1.41430	0.4304	21.9316
10	71.3860	202	1.32045	0.4647	20.9554
11	78.8804	321	1.21398	0.5710	17.9341

### 3.1.2 XRD Spectrum Analysis of SnO<sub>2</sub> Nanoparticles Synthesized Using EG as Solvent

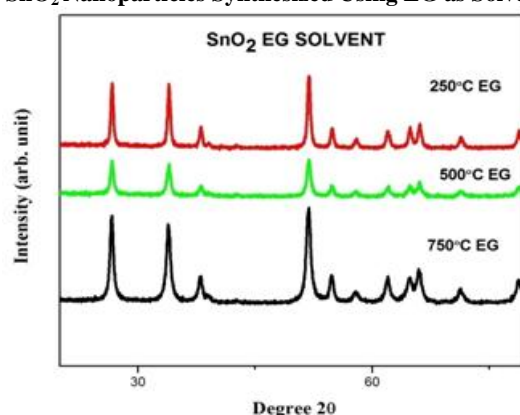


**Fig. 3.2** XRD patterns of 250 °C, 500 °C and 750 °C annealed SnO<sub>2</sub> samples synthesized using water as solvent

Fig. 3.2 shows the XRD patterns of 250 °C, 500 °C and 750 °C annealed SnO<sub>2</sub> samples synthesized using water solvent. The average crystallite size (*D*) is calculated using Scherrer's formula presented in equation (1)

$$D = \frac{0.9\lambda}{\beta \cos \theta} \quad (1)$$

Where  $\lambda$ ,  $\beta$  and  $\theta$  are the wavelength of X-ray used, full width at half maximum and Bragg's angle respectively.

From the XRD patterns of the samples it is observed that the peak are very clear and intensities are increasing with temperature this reveals that the crystallinity and the average particle size of the samples are increasing with annealing temperature. The particle size and the FWHM values and the corresponding hkl values are tabulated in the Tables 4, 5 and 6. The major peaks are in the position of 26.62°, 33.70°, 38.10°, 51.89°, 54.77°, 57.97°, 62.05°, 64.77°, 66.05°, 71.32°, 78.76° at (250°C). The major peaks are in the position of 26.69°, 33.97°, 38.08°, 51.98°, 54.81°, 57.92°, 62.08°, 64.82°, 66.09°, 71.19°, 78.81° at (500°C). The major peaks are in the position of 26.74°, 33.90°, 38.18°, 51.97°, 54.77°, 61.97°, 61.77°, 64.87°, 66.05°, 71.20°, 78.92° at (750°C). All the peaks are indexed with the JCPDS card number 72 – 1147. From the XRD pattern it revealed that the samples are in tetragonal crystal structure and it belongs to P4<sub>2</sub>/mmm space group. The average particle size of the samples are found as 14.449nm, 16.89nm, 19.03nm.

**Table 4.** Structural Parameters Of SNO<sub>2</sub> Nanoparticles Annealed With 250 °C Using EG Solvent

S.No	Peak Position	hkl value	D spacing	FWHM	Particle Size(nm)
1	26.6281	110	3.35051	0.5469	14.8637
2	33.7052	101	2.64834	0.5939	13.917
3	38.1030	200	2.36978	0.4781	17.5041
4	51.8969	211	1.76268	0.6624	13.2797
5	54.7756	220	1.67352	0.5695	15.642
6	57.9742	002	1.59424	0.7859	11.5056
7	62.0542	310	1.49865	0.6088	15.1609
8	64.7712	112	1.43882	0.6134	15.2692
9	66.0506	301	1.41721	0.6177	15.2719
10	71.3282	202	1.32258	0.7482	13.0103
11	78.7649	321	1.21661	0.7570	13.516

**Table 5.** Structural Parameters Of SNO<sub>2</sub> Nanoparticles annealed With 500 °C Using EG Solvent

S.No	Peak Position	hkl value	D spacing	FWHM	Particle Size(nm)
1	26.29	110	3.34059	0.50476	16.1089
2	33.97	101	2.63975	0.5369	15.4038
3	38.08	200	2.36511	0.4817	17.3704
4	51.98	211	1.76250	0.5416	16.2479
5	54.81	220	1.67389	0.5350	16.6524
6	57.92	002	1.59303	0.5240	17.2518
7	62.08	310	1.49578	0.5822	15.8549
8	64.82	112	1.43781	0.3923	23.8803
9	66.09	301	1.41468	0.4472	21.0955
10	71.19	202	1.32202	0.7147	13.6091
11	78.81	321	1.21345	0.8245	12.4131

**Table 6.** Structural Parameters Of SNO<sub>2</sub> Nanoparticles Annealed With 750 °C Using Eg Solvent

S.No	Peak Position	hkl value	D spacing	FWHM	Particle Size(nm)
1	26.7481	110	3.33808	0.4086	19.8972
2	33.9049	101	2.63964	0.4002	20.6614
3	38.1830	200	2.36561	0.4106	20.3855
4	51.9768	211	1.76073	0.4612	19.0775
5	54.7756	220	1.67292	0.4309	20.6718
6	61.9724	310	1.59085	0.5543	16.6424
7	61.7725	310	1.49797	0.5443	16.9224
8	64.8711	112	1.43778	0.4116	22.763
9	66.0506	301	1.41414	0.4658	20.2513
10	71.2083	202	1.32153	0.6197	15.6943
11	78.9249	321	1.21468	0.6259	16.3658

### 3.2 Optical Characterization

#### 3.2.1 FTIR Analysis

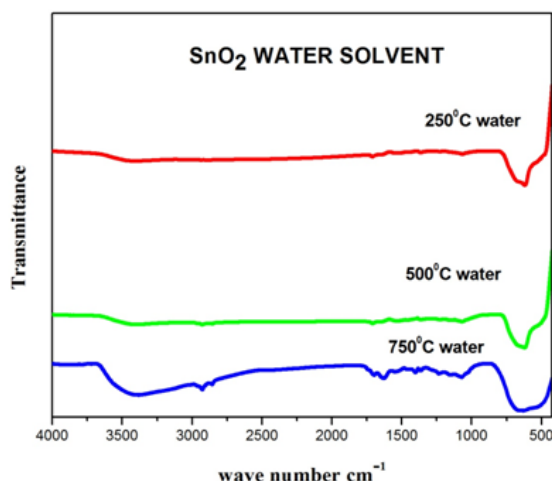


**Fig. 3.3** FTIR patterns of 250 °C, 500 °C and 750 °C annealed SnO<sub>2</sub> samples synthesized using water as solvent

FT-IR spectrum is recorded in solid phase using KBr pellet technique in the region 4000–400 cm<sup>-1</sup>. Fig. 3.3 shows the FTIR spectra of SnO<sub>2</sub> samples synthesized using water as solvent. A high intense and broad band in the range of 3500 to 3200 cm<sup>-1</sup> is assigned to O-H stretching of water molecule absorbed on the surface of SnO<sub>2</sub>. [27-34] The major IR peaks corresponding to Sn-O and O-Sn-O bond vibrations appear in the range of 700-400 cm<sup>-1</sup> in 500 °C annealed SnO<sub>2</sub>. The strong peak appeared at 620 cm<sup>-1</sup> can be assigned to [35] Sn-O-Sn. The presence of vibration peaks attributed to Sn-O bond vibration confirms the formation of SnO<sub>2</sub>.

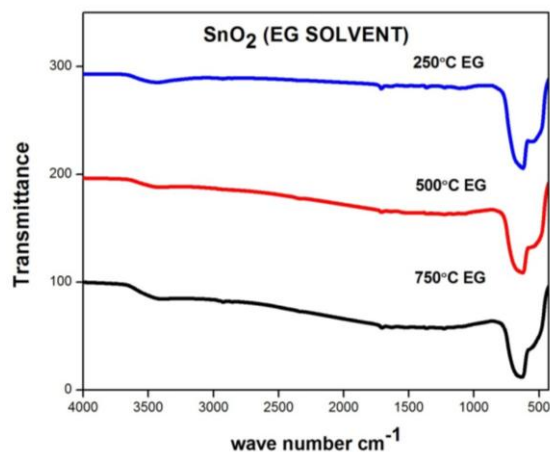


**Fig. 3.4** FTIR patterns of 250 °C, 500 °C and 750 °C annealed SnO<sub>2</sub> samples synthesized using EG as solvent

Fig. 3.4 shows the FTIR spectra of SnO<sub>2</sub> samples synthesized using EG as solvent. A high intense and broad band in the range of 3500 to 3200 cm<sup>-1</sup> is assigned to O-H stretching of water molecule absorbed on the surface of SnO<sub>2</sub>. The major IR peaks corresponding to Sn-O and O-Sn-O bond vibrations appear in the range of 700-400 cm<sup>-1</sup> in 500 °C annealed SnO<sub>2</sub>. The strong peak appeared at 620 cm<sup>-1</sup> can be assigned to Sn-O-Sn. There are some weak peaks that appeared in 2920 cm<sup>-1</sup> and 1650 cm<sup>-1</sup> associated with the surface absorbed water molecules. The peaks appeared at 1360 cm<sup>-1</sup> is related to the carbonyl group of the carboxylate ions which might remain absorbed on the surface.

### 3.2.2 UV-VIS Spectroscopy

Absorption spectroscopy is a powerful non destructive testing method for exploring the optical properties of semiconductor nanoparticles. The absorbance may depend on some of the properties like band gap, oxygen deficiency, nature of the surface and impurity centers. The spectrum shows a ultra violet cut off in the wavelength region of 200 – 230 nm. This may be related to the photo-excitation of electrons from valence band to conduction band.

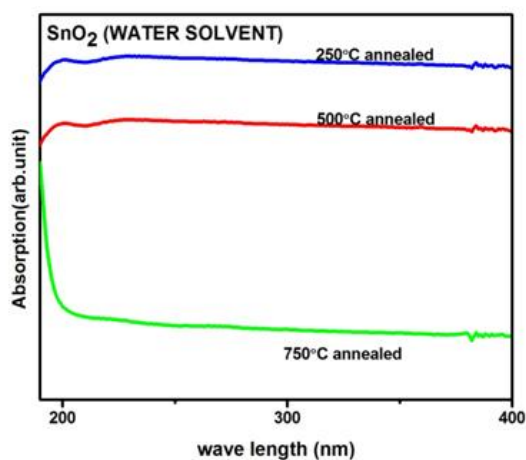


**Fig.3.5** UV-VIS Absorption spectra of SnO<sub>2</sub> samples synthesized using water as solvent

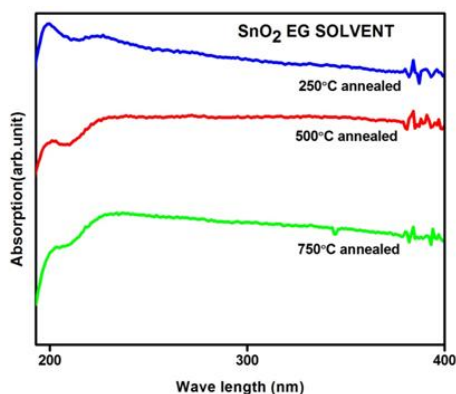


**Fig.3.6** UV-VIS Absorption spectra of SnO<sub>2</sub> samples synthesized using EG as solvent

The relationship between the absorption coefficient ( $\alpha$ ) and optical band gap can be expressed as

$$\alpha h\nu = A(h\nu - E_g)^{1/n}$$

Where  $A$  is a constant and  $h$  is Planck's constant. The exponent  $n$  depends on the type of the transition. Fig.3.7 shows the Tauc plots of SnO<sub>2</sub> samples synthesized using water and EG as solvent and the band gap values are tabulated in Table 2. [36] There is a band gap increase with increase in annealing temperature.

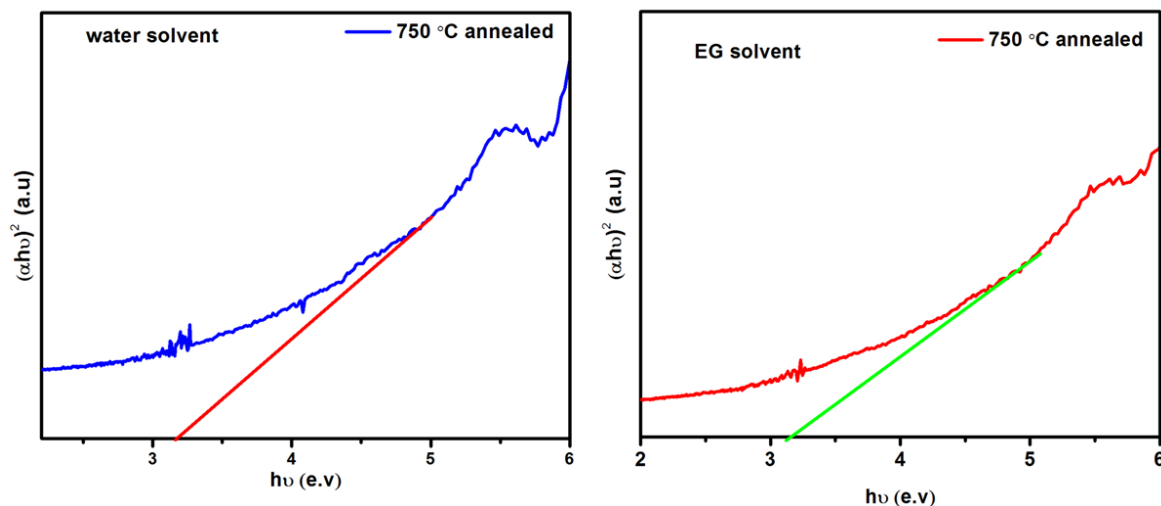


**Fig.3.7** Tauc plots of SnO<sub>2</sub> samples synthesized using water and EG as solvent.

**Table. 7** Band Gap Energy Values For SNO<sub>2</sub> Nanoparticles

Annealing temperature	Band gap energy of samples Water as solvent (eV)	Band gap energy of samples EG as solvent (eV)
250 °C	2.48	2.32
500 °C	2.79	2.59
750 °C	3.16	3.16

#### IV. Conclusion

The SnO<sub>2</sub> nanoparticles are synthesized by microwave assisted hydrothermal method. We have used water solvent and Ethelene glycol (EG) as solvents to synthesis SnO<sub>2</sub> nanoparticles. While using Water solvent, SnO<sub>2</sub> nanoparticles are in yellowish orange and while using EG solvent the SnO<sub>2</sub> nanoparticles are in grey colour. The XRD pattern of the prepared sample is indexed to the tetragonal structure of SnO<sub>2</sub>, and the calculated particle size in the range 4.566nm, 12.181nm and 19.497nm at 250,500 and 750<sup>o</sup>C respectively. From that result we can analysis that the particle sizes are increased when the annealing temperature increased. At FTIR spectrum the strong peak appeared at 620 cm<sup>-1</sup> reveals the formation of metal oxide nanoparticles. The optical band gap of SnO<sub>2</sub>nanoparticle annealed at 250<sup>o</sup>C, 500<sup>o</sup>C and 750<sup>o</sup>C are 2.48, 2.79 and 3.16eV respectively calculated from Tauc plot. Using EG as a solvent, Tin oxide was prepared and the particles are in grey colour. After the annealing colour of the samples are changed into greyish white.

The XRD pattern of the prepared sample is indexed to the tetragonal structure of SnO<sub>2</sub>, and the calculated particle size in the range 14.449nm, 16.89nm, 19.03nm at 250, 500 and 750<sup>o</sup>C respectively. From that result we can analysis that the particle sizes are increased when the annealing temperature increased. At FTIR spectrum the strong peak appeared at 620 cm<sup>-1</sup> reveals the formation of metal oxide nanoparticles. The optical band gap of SnO<sub>2</sub>nanoparticle annealed at 250<sup>o</sup>C, 500<sup>o</sup>C and 750<sup>o</sup>C are 2.32, 2.59 and 3.16eV respectively calculated from Tauc plot.

#### Acknowledgements

My heart brims with gratitude to god, my eternal guide as I submit this project. His bountiful love has enabled me to overcome all hurdles. I thank him for the amazing grace throughout my M.Sc., course. I am indebted to **my parents, brother and friends** for their loving care and constant encouragement throughout this course. Mere words cannot express my sense of gratitude so I thank them in spirit of faith. I am grateful and thankful to my staff **Mr.K.DhinakarGnam, M.Sc., M.Phil.**, for his cooperation and support towards the completion of the work. I take immense pleasure in thanking my academic guide **Mrs.K.Umamaheswari, M.Sc., M.Phil.**, Assistant Professor, Department of Physics, St. John's College, Palayamkottai, Tirunelveli for her expect guidance, inspiring discussions encouragement and moral support which helped me to accomplish this work.

#### References

- [1]. M. Ferná ndez-Garcı ´a, A. Martı ´nez-Arias, J.C. Hanson, J.A. Rodrı ´guez, Chem. Rev. 104, 4063 (2004)
- [2]. D. Varshney, K. Verma, J. Mol. Struct. 1034, 216 (2013)
- [3]. A. Azam, A.S. Ahmed, S.S. Habib, A.H. Naqvi, J. Alloys Compd. 523, 83 (2012)
- [4]. S. Das, V. Jayaraman, Prog. Mater Sci. 66, 112 (2014)

- [5]. O. Acarbas, E. Suvaci, A. Dogan, *Ceram. Int.* 33, 537 (2007)
- [6]. A. Chandra Bose, P. Thangadurai, S. Ramasamy, *Mater. Chem. Phys.* 95, 220 (2006)
- [7]. S. Liu, L. Li, W. Jiang, C. Liu, W. Ding, W. Chai, *Powder Technol.* 245, 168 (2013)
- [8]. H. Zhang, Q. He, X. Zhu, D. Pan, X. Deng, Z. Jiao, *Crys- tEngComm* 14, 3169 (2012)
- [9]. K. Manseki, T. Sugiura, T. Yoshida, *New J. Chem.* 38, 598 (2014)
- [10]. F. Gu, S.F. Wang, M.K. Lu, G.J. Zhou, D. Xu, D.R. Yuan, *J. Phys. Chem. B* 108, 8119 (2004)
- [11]. S. Sain, A. Kar, A. Patra, S.K. Pradhan, *CrystEngComm* 16, 1079 (2014)
- [12]. Z. Han, N.G.F. Li, W. Zhang, H. Zhao, Y. Qian, *Mater. Lett.* 48, 99 (2001)
- [13]. F.I. Pires, E. Joanni, R. Savu, M.A. Zaghete, E. Longo, J.A. Varela, *Mater. Lett.* 62, 239 (2008)
- [14]. D.S. Wua, C.Y. Han, S.Y. Wang, N.L. Wua, I.A. Rusakova, *Mater. Lett.* 53, 155 (2002)
- [15]. T. Krishnakumar, N. Pinna, K.P. Kumari, K. Perumal, R. Jaya- Prakash, *Mater. Lett.* 62, 3437 (2008)
- [16]. H.E. Wang, L.J. Xi, R.G. Maa, Z.G. Lu, C.Y. Chung, I. Bello, J.A. Zapien, *J. Solid State Chem.* 190, 104 (2012)
- [17]. P. Chetri, A. Choudury, *Phys. E* 47, 257 (2013)
- [18]. Y. Wang, J.Y. Lee, *J. Power Sources* 144, 220 (2005) This heading is not assigned a number.
- [19]. S. Das, A. K. Mukhopadhyay, S. Datta and D. Basu, "Pros- pects of Microwave Processing: An Overview," *Bulletin of Materials Science*, Vol. 32.
- [20]. Yang H, Hu Y, Tang A, et al. Synthesis of tin oxide nanoparticles by mechanochemical reaction. *J Alloys Compd*, 363: 276–279, 2004.
- [21]. Pan ZW, Dai ZR, Wang ZL. Nanobelts of semiconducting oxides. *Science* 2001, 291: 1947–1949.
- [22]. Baik NS, Sakai G, Miura N, et al. Preparation of stabilized nanosized tin oxide particles by hydrothermal treatment. *J Am Ceram Soc*, 83: 2983–2987, 2000.
- [23]. Song KC, Kang Y. Preparation of high surface area tin oxide powders by a homogeneous precipitation method. *Mater Lett*, 42: 283–289, 2000.
- [24]. Zhu J-J, Zhu J-M, Liao X-H, et al. Rapid synthesis of nanocrystalline SnO<sub>2</sub> powders by microwave heating method. *Mater Lett*, 53: 12–19, 2002.
- [25]. Wu D-S, Han C-Y, Wang S-Y, et al. Microwave-assisted solution synthesis of SnO<sub>2</sub> nanocrystallites. *Mater Lett*, 53: 155–159, 2002.
- [26]. Pires FI, Joanni E, Savu R, et al. Microwave-assisted hydrothermal synthesis of nanocrystalline SnO<sub>2</sub> powders. *Mater Lett* 62: 239–242. 2008.
- [27]. Krishna M, Komarneni S. Conventional- vs microwave-hydrothermal synthesis of tin oxide, SnO<sub>2</sub> nanoparticles. *Ceram Int*, 35: 3375–3379, 2009.
- [28]. Nehru LC, Swaminathan V, Sanjeeviraja C. Rapid synthesis of nanocrystalline ZnO by a microwave- assisted combustion method. *Powder Technol*, 226: 29–33, 2012.
- [29]. Ristić M, Ivanda M, Popović S, et al. Dependence of nanocrystalline SnO<sub>2</sub> particle size on synthesis route. *J Non-Cryst Solids*, 303: 270–280, 2002.
- [30]. Wu J-J, Liu S-C. Catalyst-free growth and characterization of ZnO nanorods. *J Phys Chem B* 106: 9546–9551. 2002.
- [31]. B.C. Smith, *Infrared Spectral Interpretation: A Systematic Approach* (CRC Press, Boca Raton), 1998.
- [32]. S. Gnanam, V. Rajendran, *Dig. J. Nanomater. Bios.* 5, 699 (2010)
- [33]. S.A. Ahmed, *Solid State Commun.* 150, 2190 (2010)
- [34]. B. Behera, P. Nayaka, R.N.P. Choudhary, *J. Alloys Compd.* 436, 226 (2007)
- [35]. D.C. Sinclair, A.R. West, *J. Appl. Phys.* 66, 3850 (1989)
- [36]. A. Ullah, A. Ullah, W.S. Woo, C.W. Ahn, I.W. Kim, *Ceram. Int.* 40, 11335 (2014)